

Article

Effect of pH and Type of Stirring on the Spontaneous Precipitation of CaCO₃ at Identical Initial Supersaturation, Ionic Strength and $a(\text{Ca}^{2+})/a(\text{CO}_3^{2-})$ Ratio

Jasminka Kontrec ¹, Nenad Tomašić ², Nives Matijaković Mlinarić ¹, Damir Kralj ¹
and Branka Njegić Džakula ^{1,*}

¹ Laboratory for Precipitation Processes, Division of Materials Chemistry, Ruđer Bošković Institute, Bijenička cesta 54, 10000 Zagreb, Croatia; jasminka.kontrec@irb.hr (J.K.); nives.matijakovic@irb.hr (N.M.M.); kralj@irb.hr (D.K.)

² Faculty of Science, University of Zagreb, Horvatovac 102A, 10000 Zagreb, Croatia; ntomasic@geol.pmf.hr

* Correspondence: bnjegi@irb.hr; Tel.: +385-1-457-1343

Abstract: CaCO₃ precipitation is physical-chemical basis of biomineral formation of hard tissue (shells, skeletons) in marine calcifying organisms (=biomineralization). Processes controlling biomineralization are still not fully clarified, so the study of influence of pH on basic processes of CaCO₃ precipitation should contribute to better understanding of biomineralization under climate change. This paper reports on the effect of initial pH (pH₀) and type of stirring (mechanical and magnetical) on spontaneous precipitation and phase composition, size and morphology of spontaneously precipitated CaCO₃ formed at the identical initial supersaturation, ionic strength and $a(\text{Ca}^{2+})/a(\text{CO}_3^{2-})$ ratio. The initial pH varied in a range $8.50 \leq \text{pH}_0 \leq 10.50$ and included values relevant for mimicking the conditions related to biomineralization in marine organisms. In all systems two CaCO₃ polymorphs were found: calcite and/or vaterite. The increase of pH₀ favoured the formation of rhombohedral calcite no matter the type of stirring. This was exclusively influenced by the systems' pH₀ (other relevant initial parameters were identical). Furthermore, increase of pH₀ caused change of vaterite morphology from cauliflower-like spheroids to regular spherulites. The mechanically stirred systems produced larger calcite and vaterite particles and higher content of calcite.

Keywords: calcium carbonate; biomineralization; spontaneous precipitation; pH; stirring; calcite; vaterite



Citation: Kontrec, J.; Tomašić, N.; Matijaković Mlinarić, N.; Kralj, D.; Njegić Džakula, B. Effect of pH and Type of Stirring on the Spontaneous Precipitation of CaCO₃ at Identical Initial Supersaturation, Ionic Strength and $a(\text{Ca}^{2+})/a(\text{CO}_3^{2-})$ Ratio. *Crystals* **2021**, *11*, 1075. <https://doi.org/10.3390/cryst11091075>

Academic Editor: Francesco Capitelli

Received: 30 July 2021

Accepted: 3 September 2021

Published: 5 September 2021

Publisher's Note: MDPI stays neutral with regard to jurisdictional claims in published maps and institutional affiliations.



Copyright: © 2021 by the authors. Licensee MDPI, Basel, Switzerland. This article is an open access article distributed under the terms and conditions of the Creative Commons Attribution (CC BY) license (<https://creativecommons.org/licenses/by/4.0/>).

1. Introduction

Calcium carbonate (CaCO₃) is one of the most widespread biominerals in the marine environment. It is formed via biomineralization, in calcifying organisms (molluscs [1], corals [2], sponges [3] and foraminifera [4]). Biomineralization is a highly controlled process [5]. Precipitation processes are the physical-chemical basis of biomineralization. The main parameter controlling the precipitation of CaCO₃ is supersaturation, but other parameters such as concentration of constituent ions and dissolved carbon dioxide (CO₂) [6], presence of additives [7,8], temperature [9], pH [10], ionic strength [11] or hydrodynamics [12] are also known to influence and control CaCO₃ precipitation and consequently, together with the variety of biological constituents and processes, influence the biomineralization.

The marine calcifying organisms have evolved over millions of years within a stable environment of a narrow range of pH and temperature. The increase of CO₂ concentration in the atmosphere during the last two centuries, as direct consequence of human activity with burning of fossil fuels being one of the most detrimental, led to an increase in dissolved CO₂ levels in seas and oceans. Consequentially, this causes the change in distribution of different carbon species present in the in seas and oceans (carbonic acid—H₂CO₃, bicarbonate ions—HCO₃[−], carbonate ions—CO₃^{2−}) and decrease in ocean pH (ocean acidification). During the next century, decrease of the pH of the oceans by 0.3–0.5 units is predicted [13–16]. As a

consequence of ocean acidification, marine organisms are now forced to exist in increasingly acidic water and this raises concerns about potential extinction of species and thus massive marine biodiversity losses. Reduced skeletal growth under increased CO₂ levels has already been shown [17,18]. Calcification is known to occur between the tissue and the shell or skeleton, where pH of extrapallial fluid (in molluscs) and extracellular calcifying fluid (in corals) is from 0.5 to more than 1 units higher than in ambient sea water [19,20]. It was shown that pH of the calcifying fluid is sensitive to changes in pH of the seawater [21] and it is influenced by more than one component of the carbonate system which should be regulated in order to maintain calcification [22]. Thus, if the pH of the oceans continues to decrease, the concentration of carbonate ions can fall below the levels that are thermodynamically viable for precipitation of calcium carbonate minerals, posing a difficulty for marine organisms to maintain their hard tissue (shells, skeletons). Since the processes that control biomineralization are still not fully clarified, the investigation of basic processes and mechanisms of CaCO₃ precipitation under conditions of controlled pH will contribute to the understanding of the effects that global changes of the pH of the oceans and surface waters might have on the stability and formation of calcium carbonate shells and skeletons in marine organisms.

Many research groups [23–26] investigated the influence of pH on CaCO₃ precipitation, but in these investigations, initial supersaturation was not controlled. Namely, by changing initial pH and only keeping initial concentrations of the reactants the same, but without adjusting ionic strength and activity ratio of the constituent ions ($a(\text{Ca}^{2+})/a(\text{CO}_3^{2-})$), initial supersaturation of the system changes. Significance of the initial supersaturation on the precipitation, especially on the phase composition of the precipitate, has already been proven [27,28]. Therefore, in order to conclude about the influence of single parameter, such as pH, on calcium carbonate precipitation, the effect of this parameter must be evaluated in isolation. The importance of pH stems from the fact that CaCO₃ precipitation is a protolytic process in which, due to the change in pH, the overall equilibrium of all species in the system changes.

Our present paper was inspired by our previous work [27] and by the work of Ruiz-Agudo et al. [10], in which they investigated effect of pH on seeded calcite growth (calcite was used as seed) at identical $a(\text{Ca}^{2+})/a(\text{CO}_3^{2-})$ ratio and supersaturation. They also investigated effect of pH on spontaneous precipitation of CaCO₃ at two different pH (8.25 and 12.00), but because experiments lasted for 2 weeks it is impossible to conclude what phases of CaCO₃ initially formed in these systems and if pH had any influence on phase composition or morphology of initially formed phases. This is because during the period of two weeks transformation to the most stable CaCO₃ phase, calcite, occurred. In our previous investigation [27] it was shown that pH and supersaturation are important and interconnected parameters that could influence the morphology, polymorphic composition and/or kinetics of CaCO₃ precipitation in precipitation systems with different chemical complexities. Apart from thermodynamic parameters, our investigations also showed that hydrodynamics has significant influence on calcium carbonate precipitation processes and on properties of CaCO₃ precipitated [29].

The aim of our research was to determine how the initial pH and type of stirring influence mineralogical (polymorphic) composition, morphology and size distribution of CaCO₃ spontaneously precipitated at otherwise identical initial supersaturation, ionic strength and activity ratio of constituent ions ($a(\text{Ca}^{2+})/a(\text{CO}_3^{2-})$). We hypothesise that the change of pH as well as type of stirring will result with preferential formation of one of the CaCO₃ polymorphs that could be precipitated in the given system, and will change the morphology of the spontaneously precipitated CaCO₃. In order to achieve this aim, spontaneous precipitation of CaCO₃ was performed, which was followed by pH measurements in systems in which different types of stirring were applied. The morphology of the CaCO₃ precipitates obtained were analysed by scanning electron microscopy (SEM), while the polymorphic composition was determined by means of powder X-ray diffraction (XRD) and infrared spectroscopy (IR). Particle size was determined with Tescan Atlas software. These results should contribute to a deeper understanding of the basic mechanisms of

CaCO₃ precipitation in relation to changing pH, especially related to biomineralization in the context of climate change and ocean acidification.

2. Materials and Methods

2.1. Materials

Analytically pure chemicals CaCl₂·H₂O, NaHCO₃, NaCl and NaOH (purchased from Sigma-Aldrich, St. Louis, MS, USA as well as deionized water (conductivity less than 0.055 μS cm⁻¹) were used in all experiments.

2.2. Precipitation Experiments

Sodium bicarbonate solution was always freshly prepared by dissolving calculated mass of anhydrous NaHCO₃ in water; calcium chloride solution was prepared by adding calculated volumes of 1 mol dm⁻³ CaCl₂ stock solution into water. The initial pH of the system was adjusted by adding calculated volume of 1 mol dm⁻³ NaOH stock solution into sodium bicarbonate solution to ensure that the observed change in the kinetics were due only to changes in the initial pH and were not related to changes in solution stoichiometry or supersaturation. The ionic strength (*I_c*) of each system was fixed at 0.1 mol dm⁻³ by using 4 mol dm⁻³ NaCl stock solution. All calculated concentrations of the components in the systems are shown in Table 1.

Table 1. Initial values of pH₀, ionic strength (*I_c*), composition and activity ratio of constituent ions (*a*(Ca²⁺)/*a*(CO₃²⁻)) of the systems used in the experiments. Initial saturation ratios (*S*) of the systems with the respect to calcite and vaterite were *S_C* = 14.4 ± 0.1 and *S_V* = 7.5 ± 0.1.

pH ₀	<i>I_c</i> /mol dm ⁻³	NaHCO ₃	CaCl ₂	NaCl	NaOH	<i>a</i> (Ca ²⁺)/ <i>a</i> (CO ₃ ²⁻)
		c/mmol dm ⁻³				
8.50	0.1004	79.00	4.22	11.00	4.45	1.00
9.00	0.1001	28.30	3.75	61.70	4.75	1.00
9.50	0.1000	12.30	3.66	77.50	4.86	1.00
10.00	0.1002	7.09	3.56	83.00	4.89	1.00
10.50	0.1001	5.50	3.56	84.20	5.20	1.00

The experiments were performed in a thermostated double-walled glass vessel (Šurlan laboratory glass, Medulin, Croatia) with a 400 cm³ capacity. The vessel was tightly closed with a Teflon cover, thus minimizing the exchange of carbon dioxide between the ambient air and the reaction system. Calcium carbonate was always precipitated by mixing equal volumes (200 cm³) of CaCl₂ and NaHCO₃ solutions. The CaCl₂ solution was rapidly added into the NaHCO₃ solution.

During the precipitation, the systems were continuously stirred at a constant rate. In the first set of experiments they were stirred by means of a Teflon-coated magnetic stirring bar (magnetical stirring, Biosan, Riga, Latvia) and in the second set by means of flat-bladed stirrer with perpendicular blades (mechanical stirring, Biosan, Riga, Latvia). All experiments were carried out at 25 °C. The progress of the reaction was followed by measuring the pH of the solution using a combined glass-calomel electrode (Red Rod, Radiometer Analytical, Lyon, France) connected to a digital pH meter (PHM 290, Radiometer Analytical, Lyon, France). At the end of each experiment (approximately 30 min), the entire solution was filtered through a 0.22 μm cellulose nitrate membrane filter (Millipore Merck KGaA, Darmstadt, Germany), washed with small portions of water and dried at 105 °C.

2.3. Characterization of Precipitate

The mineralogical composition of the precipitates was analyzed by IR spectroscopy (Tensor II spectrometer, Bruker, Billerica, MA, USA) using KBr pellets (Sigma-Aldrich, St. Louis, MS, USA), and by X-ray diffraction of powdered samples (XRD) with data

collected on Philips PW 3040/60 X'Pert PRO powder diffractometer (Malvern Pananalytical, Malvern, Worcestershire, United Kingdom) using CuK α radiation ($\lambda = 1.54055 \text{ \AA}$) at 45 kV and 40 mA in Bragg-Brentano geometry. The incident beam passed through an X-ray mirror having a divergence slit of 0.5° and the diffracted beam was directed to proportional detector through a parallel plate collimator with an equatorial acceptance angle of 0.18° . Soller slits were inserted in both incident and diffracted beam paths. The powdered samples were mounted on a single silicon crystal disc cut in a way to avoid lattice planes, and thus causing no silicon diffraction and low background. The disc with a sample was inserted into the sample spinner programmed to a revolution time of 0.5 s. Step size was set to $0.02^\circ = 2\theta$ with measuring time of 0.5 seconds per step. The diffraction intensities were measured in the angular range $4^\circ \leq 2\theta \leq 65^\circ$. Data were processed on Panalytical proprietary software X'Pert HighScore Plus (Software version 2.1), and CaCO $_3$ polymorphs (calcite and vaterite) were identified according to the ICDD Powder Diffraction Files 01-072-1937 and 01-072-0506, respectively. Quantitation of phases was determined by the reference intensity ratio (RIR) method.

Particle size was determined by scanning electron microscopy (JEOL JSM-7000F, Jeol Ltd., Tokyo, Japan) and Tescan Atlas software using Feret's diameter as the characteristic dimension of particles.

The morphology of the individual crystals was observed by scanning electron microscopy (SEM) on a JEOL JSM-7000F instrument (Jeol Ltd., Tokyo, Japan). For the SEM observations, the dried samples were attached by sticky carbon tape to an aluminium stub.

2.4. Data Analyses

Calculations of the solution composition, i.e., the molar concentrations and activities of relevant ionic species, were based on the known total initial concentrations of CaCl $_2$, NaHCO $_3$, NaOH and NaCl, and initial pH. The following ionic species were considered: H $^+$, OH $^-$, CO $_3^{2-}$, HCO $_3^-$, H $_2$ CO $_3^0$, NaCO $_3^-$, CaCO $_3^0$, CaHCO $_3^+$, CaOH $^+$, CaCl $^+$, Ca $^{2+}$, Na $^+$, Cl $^-$, NaHCO $_3^0$, NaCl 0 and NaOH 0 . Calculations were performed by using an algorithm developed within this laboratory and results were compared with those obtained by VMINTEQ 3.0 when possible (available at <http://vminteq.lwr.kth.se/download/>, accessed on 30 July 2021). The supersaturations were expressed as the saturation ratio, S , defined as the square root of the quotient of the CaCO $_3$ ion activity product, $\Pi = a(\text{Ca}^{2+}) \cdot a(\text{CO}_3^{2-})$, and thermodynamic equilibrium constant of dissolution of the particular CaCO $_3$ phase, K_{sp}^0 :

$$S = (\Pi/K_{\text{sp}}^0)^{1/2} \quad (1)$$

The activity coefficients of z -valent ions, γ_z , were calculated by using a modification of the Debye-Hückel equation as proposed by Davies [30]. The detailed calculation procedure, which considers the respective protolytic equilibria and equilibrium constants, together with the charge and mass balance equations, has been described previously [7,12,31,32]. Equilibrium constants for CaCl $^+$, NaHCO $_3^0$, NaCl 0 and NaOH 0 were taken from VMINTEQ 3.0.

In all systems, initial saturation ratio (S), the initial ionic strength (I_c) and solution stoichiometry were set by calculation procedure to identical values for all systems. The initial saturation ratios (S) of the solutions/systems with the respect to calcite and vaterite were $S_C = 14.4 \pm 0.1$ and $S_V = 7.5 \pm 0.1$. With these values of S basic precondition ($S > 1$) for precipitation of vaterite and calcite was achieved. Ionic strength (I_c) was set to 0.1 mol dm^{-3} by adjusting the amount of added NaCl. The solution stoichiometry, defined as the ratio of the activities of lattice ions in solution ($a(\text{Ca}^{2+})/a(\text{CO}_3^{2-})$), was set to 1.00 by adjusting the amount of NaHCO $_3$ and CaCl $_2$ at the target pH. Initial pH of the systems varied from 8.50 to 10.50 and solution composition of each system is given in Table 1.

3. Results and Discussion

To achieve the aim of this study, the influence of initial pH (pH_0) and type of stirring on the spontaneous precipitation of CaCO $_3$ on nucleation, but also on crystal growth

and aggregation, was investigated by identifying the changes in kinetics of spontaneous precipitation of CaCO_3 and changes in phase composition, size and morphology of the isolated solid phases, separated from the suspension at predetermined time.

3.1. Precipitation Kinetics

Spontaneous precipitation of CaCO_3 was followed with pH measurements. Figure 1 shows typical time dependent change of pH (pH progress curves) during the spontaneous precipitation of calcium carbonate at 25 °C in the systems with the different initial pH in which two types of stirring were applied. In the first set of experiments, systems were stirred by means of a Teflon-coated magnetic stirring bar (magnetical stirring) (Figure 1a) and in the second set by means of flat-bladed stirrer with perpendicular blades (mechanical stirring) (Figure 1b). Figure 1c,d shows representative pH curves recorded in the systems with the initial pH 10.5, which were magnetically (Figure 1c) and mechanically (Figure 1d) stirred. The dashed lines correspond to calculated values of solubility of: vaterite ($(c_s(\text{vaterite}) = 0.123 \text{ mmol dm}^{-3}) \hat{=} (\text{pH} = 10.215)$) and calcite ($(c_s(\text{calcite}) = 0.035 \text{ mmol dm}^{-3}) \hat{=} (\text{pH} = 10.201)$).

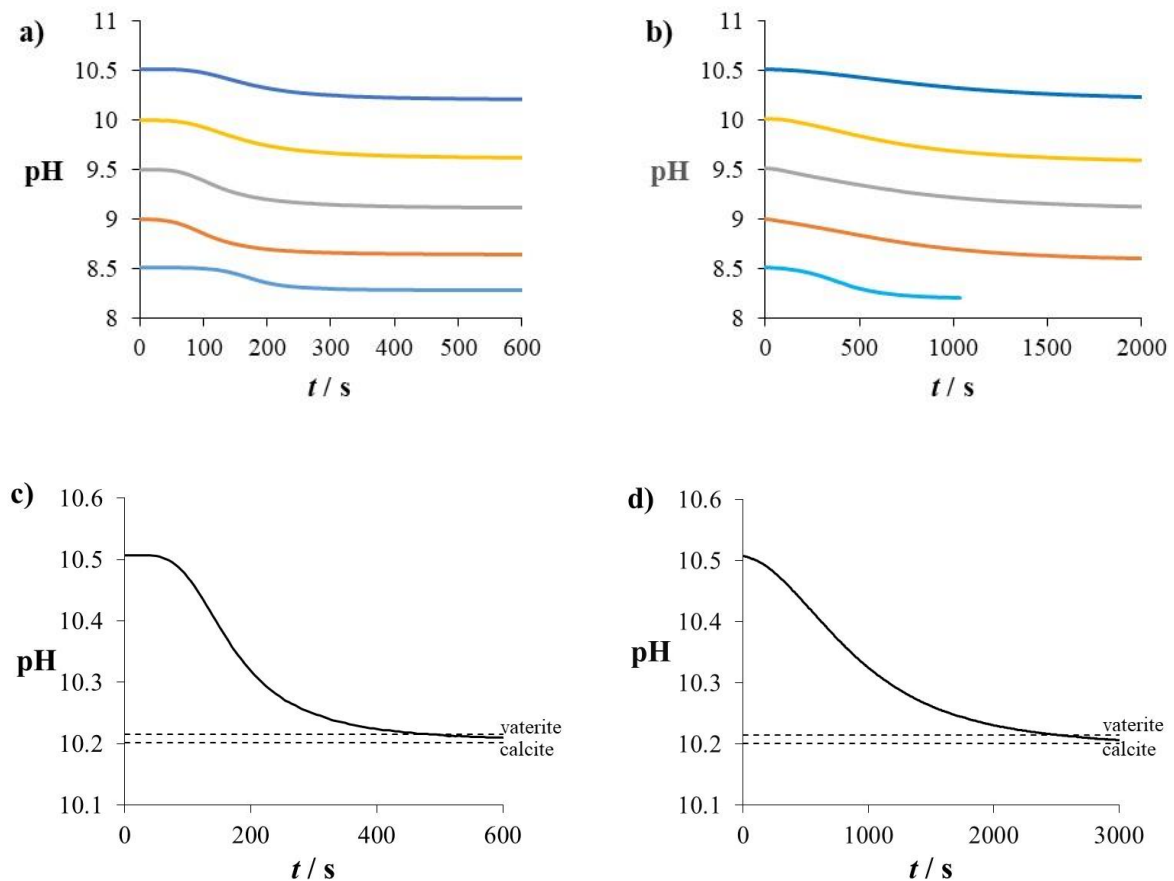


Figure 1. Progress curves, pH versus time, recorded during the spontaneous precipitation of CaCO_3 at 25 °C, in systems with different initial pH stirred by means of a Teflon-coated magnetic stirring bar—magnetical stirring ((a,c)) and flat-bladed stirrer with perpendicular blades—mechanical stirring ((b,d)), at identical initial saturation ratio ($S_C = 14.4 \pm 0.1$ and $S_V = 7.5 \pm 0.1$), ionic strength ($I_c = 0.1 \text{ mol dm}^{-3}$) and activity ratio of constituent ions ($a(\text{Ca}^{2+})/a(\text{CO}_3^{2-}) = 1.00$). The pH curves of systems with the initial pH 10.5 in magnetically (c) and mechanically (d) stirred systems in which the dashed lines correspond to calculated values of solubility of vaterite ($(c_s(\text{vaterite}) = 0.123 \text{ mmol dm}^{-3}) \hat{=} (\text{pH} = 10.215)$) and calcite ($(c_s(\text{calcite}) = 0.035 \text{ mmol dm}^{-3}) \hat{=} (\text{pH} = 10.201)$).

In order to observe only effect of pH and type of stirring on CaCO_3 precipitation, all other initial parameters were identical in all systems, meaning that the initial saturation ratio in all systems with the respect to calcite and vaterite were $S_C = 14.4 \pm 0.1$ and $S_V = 7.5 \pm 0.1$, respectively. In addition, initial ionic strength (I_c) was set to 0.1 mol dm^{-3}

and the initial activity ratio of constituent ions ($a(\text{Ca}^{2+})/a(\text{CO}_3^{2-})$) was set to 1.00 (Table 1). The precipitation was initiated by rapidly adding calcium-containing solution into the carbonate-containing solution which had preadjusted pH. Recorded pH progress curves had similar shape, indicating that the kinetics of formation of solid phases in each system were similar, regardless the initial pH or type of stirring. The first part of the pH progress curves was characterized by relatively constant pH. After certain period (induction time (t_{ind})), precipitation started, which could be observed as significant decrease of pH. In the final part of pH progress curves, changes in pH value were smaller. As seen in Figure 1c,d, in this final part of the pH curves pH falls between solubilities of vaterite and calcite, so that observed small change of pH is a consequence of two processes occurring simultaneously: vaterite dissolution and calcite growth. This composition of precipitates was confirmed with XRD and IR analysis, as discussed later. Comparing the pH curves of the systems with the same initial pH but different types of stirring, it is noticeable that in magnetically stirred systems the pH decreased faster than in case of mechanically stirred ones and achieved relatively constant pH faster (in a shorter period) indicating faster kinetics (nucleation and crystal growth) in magnetically stirred systems. To further investigate kinetics of the systems, recorded induction time was analyzed. Figure 2 shows change of the induction time (t_{ind}) with the initial pH in the precipitation systems, which were magnetically or mechanically stirred during the spontaneous precipitation of CaCO_3 at identical initial saturation ratio, ionic strength and activity ratio ($a(\text{Ca}^{2+})/a(\text{CO}_3^{2-})$).

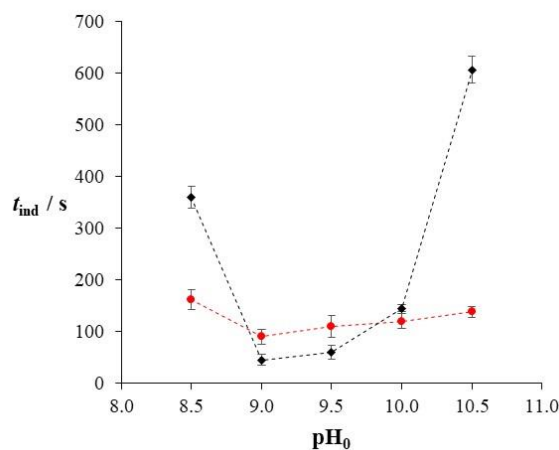


Figure 2. Change of the induction time (t_{ind}) with the initial pH in the precipitation systems, which were stirred magnetically (marked red, ●) and mechanically (marked black, ◆) during the spontaneous precipitation of CaCO_3 at identical initial saturation ratio ($S_C = 14.4 \pm 0.1$ and $S_V = 7.5 \pm 0.1$), ionic strength ($I_c = 0.1 \text{ mol dm}^{-3}$) and activity ratio of constituent ions ($a(\text{Ca}^{2+})/a(\text{CO}_3^{2-}) = 1.00$).

It can be observed that induction time in both, magnetically and mechanically stirred systems, was the shortest at pH_0 9.0 ($t_{\text{ind}}(\text{mag. sys.}) = 90 \text{ s}$ and $t_{\text{ind}}(\text{mech. sys.}) = 45 \text{ s}$) indicating maximal nucleation rate at this pH_0 . At pH_0 9.0, 9.5 and 10.0, the difference in induction time between mechanically and magnetically stirred systems is not so significant, but as pH_0 increases up to 10.5 or decreases to 8.5, the difference in induction time between magnetically and mechanically stirred systems becomes more pronounced, which is likely related to the changes in ionic species composition of system at these pH. Namely, under conditions presented in this paper, calculations of chemical speciation of each system showed that initial composition of aqueous species was relatively constant except for OH^- ions, whose concentration significantly changed at these outermost initial pH values used. This nonlinear effect of the initial pH has been reported in the literature [10]. According to Ruiz-Agudo et al. [10], who studied the effect of pH (pH range from 7.5 to 10.25) on seeded crystal growth of calcite at constant supersaturation, ionic strength and $a(\text{Ca}^{2+})/a(\text{CO}_3^{2-})$ ratio, this nonlinear trend in kinetics of CaCO_3 precipitation was also observed. In their work, crystal growth rate of calcite followed the same trend that we observed with the

nucleation rate and induction time in our investigated systems. More precisely they observed minimum crystal growth rate at pH 8.5 in seeded crystal growth of calcite. In their investigation, calcite growth rate decreased in pH range from 7.5 to 8.5, reaching its minimum at 8.5. Between 8.5 and 9.0 crystal growth rate increased (just as our nucleation rate increased) but then from 9.0 slightly decreased again parallel with the increase of pH up to 10.25 (nucleation rate in our investigation also decreased in this pH range). As can be observed in Figure 2, the nonlinear effect in our work is more pronounced in mechanically stirred systems than in magnetical ones, which can be explained by the hydrodynamics of these systems. According to Brečević et al. [33] the differences that occur between magnetically and mechanically stirred systems could be related to the fact that agitation with the magnetic stirrer is likely to produce an abrasive or grinding action as the magnetic “bob” rotates on the base of glass reactor, which results in crystal breakage and formation of higher number of smaller-sized crystals in solution, than in the case when there is no breakage of crystals, leading to shorter induction time and smaller crystals. Although their investigation was related to calcium oxalate, the same principle could be applied to calcium carbonate and our observations. Because in mechanically stirred systems there is no such grinding action that would result with additional smaller crystals in the system and with it no shortening of the induction time, the nonlinear effect of the initial pH on induction time that we observed and relate to ionic species composition of the system, becomes more pronounced.

3.2. Polymorphism

The X-ray analyses and the IR analysis of the isolated precipitates showed presence of only two solid phases, calcite and vaterite (Figures SI 1 and SI 2). Figure 3 shows change of calcite mass fraction in the precipitate with the change of the initial pH in the precipitation systems, which were stirred magnetically or mechanically during the spontaneous precipitation of CaCO_3 at identical initial saturation ratio, ionic strength and activity ratio of constituent ions ($a(\text{Ca}^{2+})/a(\text{CO}_3^{2-})$). The results indicate that, in magnetically stirred systems at pH_0 8.5 and 9.0, almost entirely vaterite precipitated. As pH_0 was further increased, the mass fraction of calcite in the precipitate also increased, even up to 50% at the highest pH_0 (10.5) investigated. Although the change in precipitate composition in mechanically stirred systems also occurred, it was less pronounced. Indeed, in the range of pH_0 from 8.5 to 10.0 the mass fraction of calcite in the precipitate was relatively constant, approximately 30%, but just as in the magnetically stirred systems, it increased significantly at the highest investigated pH_0 , up to 55%.

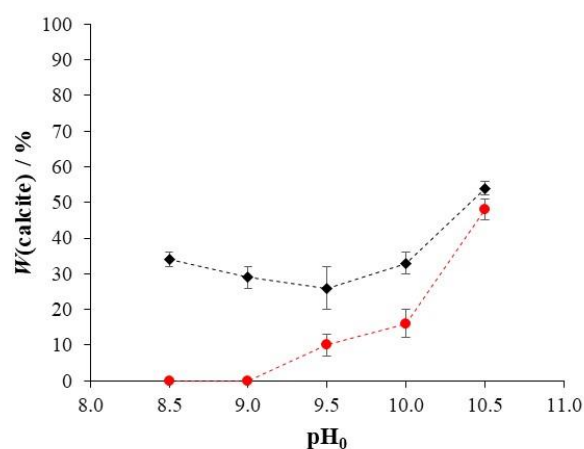


Figure 3. Mass fraction of calcite precipitated at different initial pH in the precipitation systems which were stirred) magnetically (marked red, ●) and mechanically (marked black, ◆) during the spontaneous precipitation of CaCO_3 at identical initial saturation ratio ($S_C = 14.4 \pm 0.1$ and $S_V = 7.5 \pm 0.1$), ionic strength ($I_c = 0.1 \text{ mol dm}^{-3}$) and activity ratio of constituent ions ($a(\text{Ca}^{2+})/a(\text{CO}_3^{2-}) = 1.00$).

From these data, it is possible to observe that mass fraction of calcite in the precipitate in both, magnetically and mechanically stirred systems, increases with the increase of initial pH, suggesting that higher initial pH favors formation of calcite. Considering that in all investigated systems initial supersaturation, ionic strength and $(a(\text{Ca}^{2+})/a(\text{CO}_3^{2-}))$ ratio were identical, recorded differences in precipitate composition (higher content of calcite at higher pH_0) could be mainly attributed to change in pH_0 . At $\text{pH}_0 = 10.5$, at which the greatest increase in calcite content was observed (Figure 3), concentration of hydroxyl ions (OH^-) in solution significantly increased (otherwise initial composition of aqueous species was relatively constant, as we observed by calculations of chemical speciation). Thus, we might speculate that the effect of high increase of calcite content at pH 10.5 could be related to high increase of OH^- ion concentration, which is known to facilitate Ca^{2+} dehydration and its surface adsorption and subsequent incorporation into the calcite lattice [10].

In addition to increase of calcite content with the increase of pH_0 , higher content of calcite in precipitates in mechanically stirred systems than in magnetically stirred ones was also observed. Our previous investigations showed that in the magnetically stirred systems, promotion of the vaterite formation occurred [12]. It was shown that abrasive action of magnetic bar on the glass can cause the predominant nucleation of metastable solid phases such as vaterite.

3.3. Particle Size

In Table 2, mean particle size (d_m), determined by scanning electron microscopy and Tescan Atlas software of calcite and vaterite particles isolated from precipitation systems is shown. These systems were magnetically or mechanically stirred during the spontaneous precipitation of CaCO_3 at different pH_0 , but with identical initial saturation ratio ($S_C = 14.4 \pm 0.1$ and $S_V = 7.5 \pm 0.1$), ionic strength ($I_C = 0.1 \text{ mol dm}^{-3}$) and activity ratio of constituent ions ($a(\text{Ca}^{2+})/a(\text{CO}_3^{2-}) = 1.00$).

Table 2. Mean particle size (d_m), determined by scanning electron microscopy and Tescan Atlas software, of calcite and vaterite particles isolated from precipitation systems that were magnetically or mechanically stirred during the spontaneous precipitation of CaCO_3 at different initial pH (pH_0), but identical initial saturation ratio ($S_C = 14.4 \pm 0.1$ and $S_V = 7.5 \pm 0.1$), ionic strength ($I_C = 0.1 \text{ mol dm}^{-3}$) and activity ratio of constituent ions ($a(\text{Ca}^{2+})/a(\text{CO}_3^{2-}) = 1.00$).

Type of Stirring	pH_0	Calcite	$d_m/\mu\text{m}$	Vaterite
magnetical	8.5	5.5		4.5
	9.0	4.3		4.5
	9.5	4.8		4.2
	10.0	6.1		4.5
	10.5	6.6		4.1
mechanical	8.5	19.4		24.3
	9.0	21.8		26.5
	9.5	20.9		18.6
	10.0	22.7		20.5
	10.5	26.2		21.9

It is possible to observe that the main difference in particle size did not occur within the set of samples isolated from the systems stirred with the same type of stirring, but by comparison of the samples isolated from the systems that were magnetically stirred with those that were mechanically stirred. Therefore, the main contribution to the difference in particle size can be attributed to the type of stirring. Particles (both calcite and vaterite) in the mechanically stirred systems are approximately four times larger than the particles in the magnetically stirred systems. Usually, formation of smaller crystals could be related to higher nucleation rate; higher nucleation rate indicates higher number of nuclei formed, resulting in a higher number of smaller crystals. At the same time, higher nucleation rate

indicates higher initial supersaturation, but in this case all systems had the same initial supersaturation so formation of smaller crystals can only be related to the parameters that were different (pH_0 or type of stirring) in the systems compared. In this case, the type of stirring is the key factor and as explained earlier, in Section 3.1, abrasive or grinding action of the magnetic “bob” on the base of glass reactor during stirring results in crystal breakage and formation of a higher number of smaller-sized crystals in the solution.

3.4. Morphology of Precipitated CaCO_3

In order to estimate the influence of change of pH_0 and type of stirring on CaCO_3 precipitation, the morphology of the CaCO_3 particles spontaneously precipitated in the systems was investigated by scanning electron microscopy. Scanning electron micrographs of vaterite and calcite crystals isolated from the magnetically and mechanically stirred systems at different pH_0 are shown in Figure 4. These scanning electron micrographs show that in all systems calcite crystals precipitated in their typical rhombohedral form and their morphology was not significantly affected by the change of pH_0 within the given range of pH, or by the type of stirring. However, morphology of vaterite changed significantly with the increase of pH.

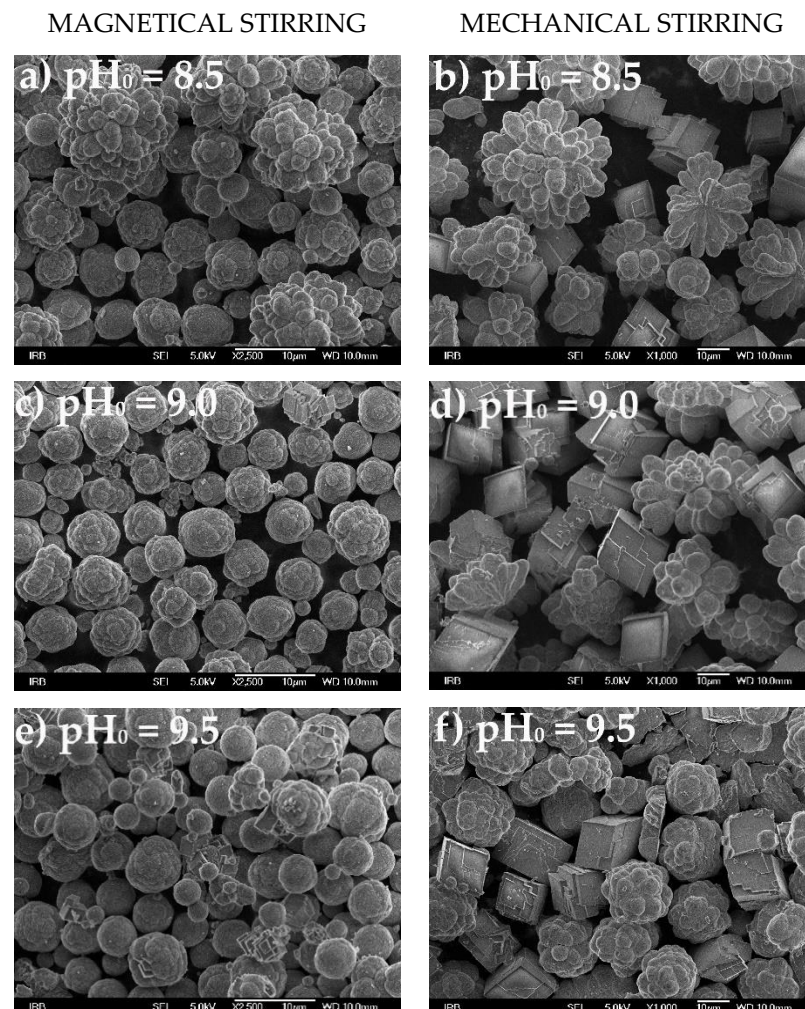


Figure 4. Cont.

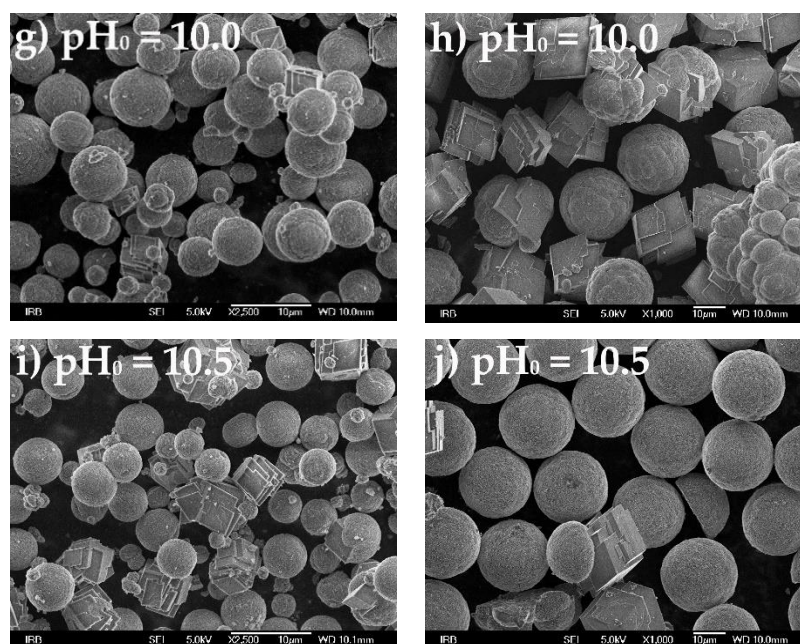


Figure 4. Scanning electron micrographs of vaterite and calcite crystals spontaneously precipitated at 25 °C in systems that were magnetically (a,c,e,g,i) and mechanically (b,d,f,h,j) stirred, with different initial pH (pH_0 from 8.5 to 10.5), at identical initial saturation ratio ($S_C = 14.4 \pm 0.1$ and $S_V = 7.5 \pm 0.1$), ionic strength ($I_c = 0.1 \text{ mol dm}^{-3}$) and activity ratio of constituent ions ($a(\text{Ca}^{2+})/a(\text{CO}_3^{2-}) = 1.00$). Scale bar is 10 μm .

In magnetically stirred systems (Figure 4a,c,e,g,i) at $\text{pH}_0 = 8.5$ (Figure 4a), two types of morphologies of vaterite could be observed: (1) vaterite particles as spherulitic aggregates and (2) vaterite particles in the form of spheroid aggregates, having the overall shape of cauliflowers. At $\text{pH}_0 = 9.0$ (Figure 4c) vaterite in the form of cauliflowers could still be observed, but was less present than in the system with $\text{pH}_0 = 8.5$. As pH_0 continued to increase, the amount of vaterite particles in the form of cauliflowers decreased so that at the highest pH_0 (10.5) (Figure 4i), no cauliflowers could be observed but only spherulites were found. The same type of morphology of vaterite (spherulites and cauliflowers) was also observed in mechanically stirred systems (Figure 4b,d,f,h,j). In fact, the change of morphology caused by increase of pH_0 followed the same trend as in magnetically stirred systems—as pH_0 increased, the amount of vaterite particles in the form of cauliflowers decreased and amount of vaterite in the form of spherulites increased. At highest pH_0 used (10.5) (Figure 4j) only regular spherulites of vaterite (besides calcite) were observed. Furthermore, the only difference in vaterite morphology that was observed between magnetically and mechanically stirred systems was related to the amount of vaterite particles that were in the form of regular spherulites. Namely, at the $\text{pH}_0 = 8.5$, in mechanically stirred system (Figure 4b), just a very small amount of vaterite was in the form of spherulites and vaterite was dominantly in the form of cauliflowers, while in the magnetically stirred system with the same pH_0 (8.5), the number of vaterite particles in the form of spherulites was visibly higher.

From these observations, it is possible to conclude that the main effect on vaterite morphology was caused by the change of pH_0 and that higher pH favours formation of vaterite particles in the form of spherulites. This is in agreement with the previous investigations in which spherulites were always formed under the high pH conditions [8,28,34,35] while cauliflowers were formed at lower pH [25]. As found earlier [8], these vaterite spherulites are aggregates of crystallites 25–35 nm in size, while cauliflower-like structures may result from the reaggregation of the vaterite spherulites, as suggested by Zhou et al. [25]. It has been extensively reported that vaterite assembles in numerous shapes depending on chemical and physical parameters governing precipitation [36–38]. Boyjoo et al. [39] in their overview considered key parameters (pH, method, additive, and concentration) influencing CaCO_3

morphology and found that solution pH has a drastic effect on vaterite morphology, but it should be noted that in their overview they compared results from different investigations in which, besides pH, parameters governing precipitation such as supersaturation, concentration ratio of reactants or additives, also varied. In this case, it is difficult to discriminate contribution of individual parameters to morphology of precipitated vaterite. Nevertheless, the trend of vaterite precipitating in the form of spherulites in the systems with higher pH could be observed.

This trend was confirmed with results presented in this paper, and because supersaturation was identical in all the systems it is possible to contribute all the effects exclusively to pH change.

4. Conclusions

The influence of initial pH and type of stirring on kinetics, phase composition, size and morphology of spontaneously precipitated CaCO_3 were investigated. Considering that supersaturation, ionic strength and activity ratio of constituent ions $a(\text{Ca}^{2+})/a(\text{CO}_3^{2-})$ influence the phase composition and morphology of the precipitated CaCO_3 , initial values of these parameters were the same in all experiments, which enabled us to attribute all observed effects just to initial pH or to type of stirring.

This research showed that:

- Induction time of CaCO_3 spontaneous precipitation in magnetically and mechanically stirred systems depends on initial pH and type of stirring. The effects of pH on induction time were more pronounced in mechanically stirred systems.
- The increase of initial pH favours the formation of calcite no matter the type of stirring. Concurrently, comparison of samples isolated from the systems with the same initial pH, but different type of stirring, showed that mass fraction of calcite was higher in the samples isolated from the systems that were mechanically stirred. This leads to the conclusion that magnetical stirring favours formation of vaterite while mechanical stirring favours formation of calcite.
- Size of crystals depends on the type of stirring used; both calcite and vaterite crystals were larger in the mechanically stirred systems than the crystals isolated from the magnetically stirred systems.
- Type of stirring did not influence the morphology of precipitated CaCO_3 crystals. The main factor contributing to the change of morphology was pH. Morphology of calcite crystals did not significantly change with the increase of pH (calcite remained in the form of rhombohedra), but by increasing pH the morphology of the vaterite crystals changed from cauliflower-like spheroids to regular spherulites.

These results clearly indicate significant contribution of initial pH in overall effect of all parameters relevant for precipitation processes and biomineralization, especially in the context of climate change and ocean acidification.

Supplementary Materials: The following are available online at <https://www.mdpi.com/article/10.3390/cryst11091075/s1>, Figure SI 1: FTIR spectra of calcium carbonate precipitated at different initial pH in the precipitation systems that were stirred (a) magnetically and (b) mechanically during the spontaneous precipitation of CaCO_3 at identical initial saturation ratio ($S_C = 14.4 \pm 0.1$ and $S_V = 7.5 \pm 0.1$), ionic strength ($I_C = 0.1 \text{ mol dm}^{-3}$) and activity ratio of constituent ions ($a(\text{Ca}^{2+})/a(\text{CO}_3^{2-}) = 1.00$). V—vaterite, C—calcite; Figure SI 2: PXRD patterns of calcium carbonate precipitated at different initial pH in the precipitation systems that were stirred (a) magnetically and (b) mechanically during the spontaneous precipitation of CaCO_3 at identical initial saturation ratio ($S_C = 14.4 \pm 0.1$ and $S_V = 7.5 \pm 0.1$), ionic strength ($I_C = 0.1 \text{ mol dm}^{-3}$) and activity ratio of constituent ions ($a(\text{Ca}^{2+})/a(\text{CO}_3^{2-}) = 1.00$). V—vaterite, C—calcite.

Author Contributions: Conceptualization, B.N.D.; methodology B.N.D. and J.K.; validation, B.N.D. and J.K.; formal analysis, J.K., N.T. and N.M.M.; investigation, B.N.D., J.K., N.T. and N.M.M.; resources, D.K.; data curation, B.N.D., J.K., N.T. and N.M.M.; writing—original draft preparation, B.N.D., J.K., N.T., N.M.M. and D.K.; writing—review and editing, B.N.D.; visualization, J.K.; supervi-

sion, D.K.; project administration, D.K.; funding acquisition, D.K. All authors have read and agreed to the published version of the manuscript.

Funding: This research received no external funding.

Institutional Review Board Statement: Not applicable.

Informed Consent Statement: Not applicable.

Data Availability Statement: Data is contained within the article or supplementary material.

Acknowledgments: This work has been supported in part (B.N.D., J.K., N.M.M. and D.K.) by Croatian Science Foundation under the project IP-2013-11-5055. The authors acknowledge the helpful comments and suggestions of anonymous reviewers.

Conflicts of Interest: The authors declare no conflict of interest.

References

1. Checa, A.G. Physical and biological determinants of the fabrication of Molluscan shell microstructures. *Front. Mar. Sci.* **2018**, *5*, 353. [[CrossRef](#)]
2. Veron, J.E.N. Corals: Biology, Skeletal Deposition, and Reef-Building. In *Encyclopedia of Modern Coral Reefs*; Hopley, D., Ed.; Encyclopedia of Earth Sciences; Springer: Dordrecht, The Netherlands, 2011; pp. 275–281.
3. Uriz, M.J. Mineral skeletogenesis in sponges. *Can. J. Zool.* **2006**, *84*, 322–356. [[CrossRef](#)]
4. Jacob, D.E.; Wirth, R.; Agbaje, O.B.A.; Branson, O.; Eggins, S.M. Planktic foraminifera form their shells via metastable carbonate phases. *Nat. Commun.* **2017**, *8*, 1265. [[CrossRef](#)]
5. Mann, S. *Biom mineralization: Principles and Concepts in Bioinorganic Materials Chemistry*; Oxford University Press: New York, NY, USA, 2001; ISBN 0198508824.
6. Carlson, C.A.; Bates, N.R.; Hansell, D.A.; Steinberg, D.K. Carbon Cycle. In *Encyclopedia of Ocean Sciences*; Elsevier: Amsterdam, The Netherlands, 2001; pp. 390–400.
7. Njegić-Džakula, B.; Brečević, L.; Falini, G.; Kralj, D. Calcite Crystal Growth Kinetics in the Presence of Charged Synthetic Polypeptides. *Cryst. Growth Des.* **2009**, *9*, 2425–2434. [[CrossRef](#)]
8. Brečević, L.; Nöthig-Laslo, V.; Kralj, D.; Popović, S. Effect of divalent cations on the formation and structure of calcium carbonate polymorphs. *J. Chem. Soc. Faraday Trans.* **1996**, *92*, 1017–1022. [[CrossRef](#)]
9. Jie, P.; Zhiming, L. Influence of temperature on microbially induced calcium carbonate precipitation for soil treatment. *PLoS ONE* **2019**, *14*, e0218396.
10. Ruiz-Agudo, E.; Putnis, C.V.; Rodriguez-Navarro, C.; Putnis, A. Effect of pH on calcite growth at constant $a\text{Ca}^{2+}/a\text{CO}_3^{2-}$ ratio and supersaturation. *Geochim. Cosmochim. Acta* **2011**, *75*, 284–296. [[CrossRef](#)]
11. Zuddas, P.; Mucci, A. Kinetics of Calcite Precipitation from Seawater: II. The Influence of the Ionic Strength. *Geochim. Cosmochim. Acta* **1998**, *62*, 757–766. [[CrossRef](#)]
12. Kralj, D.; Brečević, L.; Nielsen, A.E. Vaterite growth and dissolution in aqueous solution I. Kinetics of crystal growth. *J. Cryst. Growth* **1990**, *104*, 793–800. [[CrossRef](#)]
13. Doney, S.C.; Fabry, V.J.; Feely, R.A.; Kleypas, J.A. Ocean Acidification: The Other CO₂ Problem. *Ann. Rev. Mar. Sci.* **2009**, *1*, 169–192. [[CrossRef](#)] [[PubMed](#)]
14. Feely, R.A.; Doney, S.C.; Cooley, S.R. Ocean Acidification: Present Conditions and Future Changes in a High-CO₂ World. *Oceanography* **2009**, *22*, 36–47. [[CrossRef](#)]
15. Tans, P. An Accounting of the Observed Increase in Oceanic and Atmospheric CO₂ and the Outlook for the Future. *Oceanography* **2009**, *22*, 26–35. [[CrossRef](#)]
16. Key, R.M.; Kozyr, A.; Sabine, C.L.; Lee, K.; Wanninkhof, R.; Bullister, J.L.; Feely, R.A.; Millero, F.J.; Mordy, C.; Peng, T.-H. A global ocean carbon climatology: Results from Global Data Analysis Project (GLODAP). *Global Biogeochem. Cycles* **2004**, *18*, GB4031. [[CrossRef](#)]
17. Kroeker, K.J.; Kordas, R.L.; Crim, R.N.; Singh, G.G. Meta-analysis reveals negative yet variable effects of ocean acidification on marine organisms. *Ecol. Lett.* **2010**, *13*, 1419–1434. [[CrossRef](#)] [[PubMed](#)]
18. Gazeau, F.; Quiblier, C.; Jansen, J.M.; Gattuso, J.-P.; Middelburg, J.J.; Heip, C.H.R. Impact of elevated CO₂ on shellfish calcification. *Geophys. Res. Lett.* **2007**, *34*, L07603. [[CrossRef](#)]
19. Ries, J.B. A physicochemical framework for interpreting the biological calcification response to CO₂-induced ocean acidification. *Geochim. Cosmochim. Acta* **2011**, *75*, 4053–4064. [[CrossRef](#)]
20. McConnaughey, T.A.; Gillikin, D.P. Carbon isotopes in mollusk shell carbonates. *Geo-Mar. Lett.* **2008**, *28*, 287–299. [[CrossRef](#)]
21. Kubota, K.; Yokoyama, Y.; Ishikawa, T.; Suzuki, A.; Ishii, M. Rapid decline in pH of coral calcification fluid due to incorporation of anthropogenic CO₂. *Sci. Rep.* **2017**, *7*, 7694. [[CrossRef](#)]
22. Comeau, S.; Tambutté, E.; Carpenter, R.C.; Edmunds, P.J.; Evensen, N.R.; Allemand, D.; Ferrier-Pagès, C.; Tambutté, S.; Venn, A.A. Coral calcifying fluid pH is modulated by seawater carbonate chemistry not solely seawater pH. *Proc. R. Soc. B Biol. Sci.* **2017**, *284*, 20161669. [[CrossRef](#)]

23. Korchef, A.; Touaibi, M. Effect of pH and temperature on calcium carbonate precipitation by CO₂ removal from iron-rich water. *Water Environ. J.* **2020**, *34*, 331–341. [[CrossRef](#)]
24. Rodriguez-Blanco, J.D.; Shaw, S.; Bots, P.; Roncal-Herrero, T.; Benning, L.G. The role of pH and Mg on the stability and crystallization of amorphous calcium carbonate. *J. Alloys Compd.* **2012**, *536* (Suppl. S1), S477–S479. [[CrossRef](#)]
25. Zhou, G.-T.; Yao, Q.-Z.; Fu, S.-Q.; Guan, Y.-B. Controlled crystallization of unstable vaterite with distinct morphologies and their polymorphic transition to stable calcite. *Eur. J. Mineral.* **2010**, *22*, 259–269. [[CrossRef](#)]
26. Tobler, D.J.; Rodriguez Blanco, J.D.; Sørensen, H.O.; Stipp, S.L.S.; Dideriksen, K. Effect of pH on Amorphous Calcium Carbonate Structure and Transformation. *Cryst. Growth Des.* **2016**, *16*, 4500–4508. [[CrossRef](#)]
27. Buljan Meić, I.; Kontrec, J.; Domazet Jurašin, D.; Njegić Džakula, B.; Štajner, L.; Lyons, D.M.; Dutour Sikirić, M.; Kralj, D. Comparative Study of Calcium Carbonates and Calcium Phosphates Precipitation in Model Systems Mimicking the Inorganic Environment for Biomineralization. *Cryst. Growth Des.* **2017**, *17*, 1103–1117. [[CrossRef](#)]
28. Njegić-Džakula, B.; Falini, G.; Brečević, L.; Skoko, Ž.; Kralj, D. Effects of initial supersaturation on spontaneous precipitation of calcium carbonate in the presence of charged poly-l-amino acids. *J. Colloid Interface Sci.* **2010**, *343*, 553–563. [[CrossRef](#)] [[PubMed](#)]
29. Mlinarić, N.M.; Kontrec, J.; Džakula, B.N.; Falini, G.; Kralj, D. Role of hydrodynamics, li+ addition and transformation kinetics on the formation of plate-like {001} calcite crystals. *Crystals* **2021**, *11*, 250. [[CrossRef](#)]
30. Davis, C.W. *Ion Association*; Butterworths: London, UK, 1962.
31. Kralj, D.; Brečević, L.; Kontrec, J. Vaterite growth and dissolution in aqueous solution III. Kinetics of transformation. *J. Cryst. Growth* **1997**, *177*, 248–257. [[CrossRef](#)]
32. Kralj, D.; Brečević, L.; Nielsen, A.E. Vaterite growth and dissolution in aqueous solution II. Kinetics of dissolution. *J. Cryst. Growth* **1994**, *143*, 269–276. [[CrossRef](#)]
33. Brečević, L.; Kralj, D.; Garside, J. Factors influencing the distribution of hydrates in calcium oxalate precipitation. *J. Cryst. Growth* **1989**, *97*, 460–468. [[CrossRef](#)]
34. Andreassen, J.P.; Hounslow, M.J. Growth and aggregation of vaterite in seeded-batch experiments. *AIChE J.* **2004**, *50*, 2772–2782. [[CrossRef](#)]
35. Nehrke, G.; Van Cappellen, P. Framboidal vaterite aggregates and their transformation into calcite: A morphological study. *J. Cryst. Growth* **2006**, *287*, 528–530. [[CrossRef](#)]
36. Andreassen, J.-P. Formation mechanism and morphology in precipitation of vaterite—Nano-aggregation or crystal growth? *J. Cryst. Growth* **2005**, *274*, 256–264. [[CrossRef](#)]
37. Meldrum, F.C.; Cölfen, H. Controlling Mineral Morphologies and Structures in Biological and Synthetic Systems. *Chem. Rev.* **2008**, *108*, 4332–4432. [[CrossRef](#)] [[PubMed](#)]
38. Andreassen, J.P.; Beck, R.; Nergaard, M. Biomimetic type morphologies of calcium carbonate grown in absence of additives. *Faraday Discuss.* **2012**, *159*, 247–261. [[CrossRef](#)]
39. Boyjoo, Y.; Pareek, V.K.; Liu, J. Synthesis of micro and nano-sized calcium carbonate particles and their applications. *J. Mater. Chem. A* **2014**, *2*, 14270–14288. [[CrossRef](#)]